In-line microfiber-assisted Mach-Zehnder interferometer for microfluidic highly sensitive measurement of salinity

Nanjie Xie, Hao Zhang, Bo Liu, Haifeng Liu, Ting Liu, Chao Wang

***Abstract*—We present a microfluidic U-shaped micro-cavity sensor by splicing a segment of microfiber of a few hundred micrometers in length tapered from a single-mode fiber (SMF) between two SMFs with predesigned lateral offset for highly sensitive salinity measurement. The proposed sensing probe serves as an in-line microfiber-assisted Mach-Zehnder interferometer (MAMZI) with an ultra-high refractive index sensitivity of 10^4 nm/RIU. Three Mach-Zehnder interferometer structures with different cavity lengths of 351.82 μm, 242.56 μm and 181.31 μm are fabricated, by which microfluidic sensing systems are established for in-line measurement of sodium chloride (NaCl) solution. Experimental results indicate that the detection limit of NaCl solution is as low as 4×10^{-3} wt% and the response time is less than 15 s, which would make the MAMZI-based microfluidic measuring system play an important role in label-free biological and chemical detection applications.**

***Index Terms*—Microfluidic sensing; Salinity sensor; Fiber-optic interferometer; Mach-Zehnder interferometer; Microfiber**

I. Introduction

In recent years, label-free detection of biological and chemical analytes has attracted growing research interests to achieve highly-sensitive and fast-response trace detection of femtoliter to nanoliter samples. The integration of optics and microfluidics known as optofluidics provides an efficient approach to achieve in-line microfluidic detection of biochemical analysis with low sample and reagent consumption, good portability as well as automated manipulation [1-4], and a good variety of optofluidic devices have been demonstrated in the past decade, including four-channel-integrated Young interferometer chip [5], optofluidic Mach-Zehnder interferometer [6, 7], and optofluidic surface-enhanced Raman scattering (SERS) platform [8].

Measurement of Sodium Chloride (NaCl) in aqueous solution known as salinity has been intensively investigated for practical applications in the fields of oceanography, manufacture industry, and quality monitoring of water resources [9, 10]. However, conventional electrical-conductivity-based salinity solution measurement techniques are vulnerable to electrical interference, which makes them unable to meet the demand for high-accuracy and high-resolution measurement in biological and chemical applications [11]. Owing to their desirable advantages such as compact structure, immunity to electromagnetic interference and ease of fabrication, fiber sensors have become the promising candidates to fulfill the salinity determination by measuring the light intensity or refractive index (RI) variation when the aqueous solution concentration changed. Consequently, various salinity fiber sensors based on the RI change of the analytes have been developed, including fiber gratings [12-15], fiber interferometers [16-19], tapered fiber [20, 21], optical fiber surface plasma resonance (SPR) [22, 23] and photonic crystal fiber (PCF) [24, 25], etc. It should be noted that the RI sensitivities of certain wavelength-interrogated fiber interferometers and typical fiber grating sensors are about several hundred nanometers per refractive index unit (RIU) and the sensing probe are directly immersed into a sample sin, which implies that their detection sensitivity of salinity is relatively low and sample consumption is very large. To overcome the above difficulty, SPR- and PCF-based salinity sensors have been proposed to improve the detection sensitivities due to their outstanding detection limits of RI reaching to 10^{-6} (RIU). However, for SPR sensor schemes, a thin metallic layer of a few tens of nanometers in thickness is usually required to be deposited on the fiber surface for enhanced evanescent field to meet the plasmonic resonance condition. And meanwhile the PCF-integrated optofluidic refractometers have the difficulty in loading fluid samples into their cross-sectional tiny air holes, which makes the response time as long as a few minutes. Besides, both of these two kinds of sensor schemes require laborious sensor fabrication procedures and relatively high cost.

We have proposed a microfluidic microfiber-assisted Mach-Zehnder interferometer (MAMZI) with its interference arms constituted by a microfiber of a few hundreds micrometers in length and a U-shaped micro-cavity as the sample carrier in this

Manuscript received JUNE 19, 2018. This work was jointly supported by the National Natural Science Foundation of China under Grant Nos. 11774181, 61727815, 11274182, 61377095 and 11004110, Science & Technology Support Project of Tianjin under Grant No. 16YFZCSF00400, and the 863 National High Technology Program of China under Grant No. 2013AA014201. (Corresponding author: Hao Zhang)

N. Xie, H. Zhang, B. Liu, H. Liu, and T. Liu are with Tianjin Key Laboratory of Optoelectronic Sensor and Sensing Network Technology, Institute of Modern Optics, Nankai University, Tianjin 300350, China. (e-mail: 1583490928@qq.com; haozhang@nankai.edu.cn; liubo@nankai.edu.cn; hfliu@mail.nankai.edu.cn; 1349224572@qq.com)

C. Wang is with School of Engineering and Digital Arts, University of Kent, Canterbury CT2 7NT, United Kingdom. (e-mail: c.wang@kent.ac.uk)

paper. The direct interaction between operation light and analytes equips our proposed fiber interferometer with ultra-high RI sensitivity [26, 27]. The proposed sensor structure is easy to fabricate as only fiber tapering and splicing procedures are required. A microfluidic sensing system is established by using the proposed microfiber-assisted fiber interferometer as the key sensor element, showing a wavelength sensitivity up to 24.19 nm/(1 wt%) and the response time of less than 15 seconds for NaCl solution as a typical analyte Experimental results indicate that our proposed interferometer could work as a promising candidate for related label-free biological and chemical detection applications.

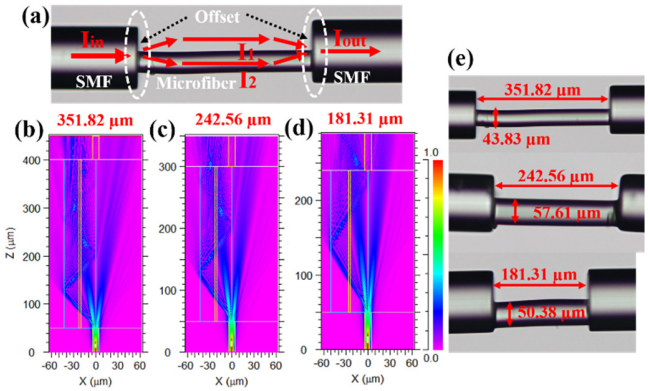

Fig. 1. (a) Microscopic image of the fabricated MAMZI; (b)-(d) Simulated electric field intensity evolution of the MAMZIs with respective cavity length of 351.82 μm, 242.56 μm and 181.31 μm when the ambient environment is air; (e) Microscopic images of the MAMZIs with different cavity lengths and microfiber diameters.

II. Fabrication Procedure of the MAMZI and Operation Principle

Fig. 1(a) is the microscopic image of the fabricated MAMZI structure. The microfiber could be obtained by employing flame scanning tapering technique to reduce the diameter of the standard SMF down to about 40 to 60 micrometers. A commercial optical fiber splicer (Fujikura FSM-60s, Japan) is utilized to splice the microfiber with the two SMFs which could lead the incident light in and out, respectively. The important related splicing parameters have been reported in our previous work [27]. And in order to optimize the spectral fringe visibility, a large lateral offset of about one half of the microfiber diameter is deliberately introduced between the cores of the microfiber and the SMF. If the lateral offset between the microfiber and SMFs equals to one diameter of the microfiber, the fiber cores of both SMFs will be completely exposed to the air. In this case the spectral interference would result from Fabry-Pérot mechanism instead. However, since the refractive index sensitivity of a Fabry-Pérot interferometer is much lower than its Mach-Zehnder counterpart, and moreover the fiber facet damaging introduced during the fiber splicing process will inevitably reduce the facet reflectivity, in this study Mach-Zehnder structure is employed as the sensor component. The detailed fabrication procedure of our proposed MAMZI is presented in our earlier work [28]. As schematically depicted in Figure 1(a), the incident light I_{in} is separated into two branches I_1 and I_2 at the left splicing joint between the lead-in SMF and the microfiber, which would continue propagating through the U-shaped micro-cavity and the microfiber, respectively. Owing to the existence of refractive index difference Δn_{eff} between the micro-cavity index n_1 and the microfiber index n_2, the two beams would experience totally different optical paths. When only dual mode interference which would occur at the lead-out SMF after the two portion of light re-combining at the right splicing joint is taken into account, the output light intensity I_{out} which is related to the wavelength could be described as:

$$I(\lambda) = I_1 + I_2 + 2\sqrt{I_1 I_2}\cos(\Delta\varphi) \qquad (1)$$

where $\Delta\varphi = 2\pi L(n_1 - n_2)/\lambda = 2\pi L\Delta n_{eff}/\lambda$ is defined by the phase difference between the two branches of light, and L is the physical interference length. As $\Delta\varphi = (2n+1)\pi$, where n is an integer, I_{out} would be the minimum value. Consequently, the nth order central wavelength λ_n of interference dip could be expressed by:

$$\lambda_m = 2\Delta n_{eff} L/(2m+1) \qquad (2)$$

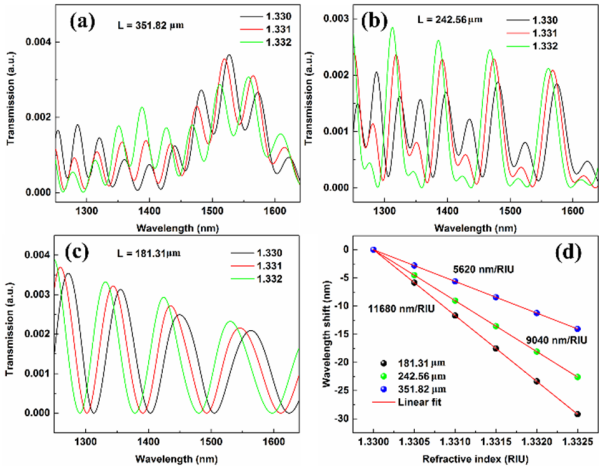

Fig. 2. (a)-(c) Simulated transmission spectra of the three MAMZIs with respective cavity lengths of 351.82 μm, 242.56 μm and 181.31 μm as the ambient environment RI varies from 1.33 to 1.332; (d) Calculated RI sensitivities of the three MAMZIs as the ambient environment RI varies from 1.33 to 1.3325.

Three microfiber-assisted MZIs with cavity lengths of 351.82 μm, 242.56 μm and 181.31 μm are fabricated by repeating the above fabrication procedure, as depicted in Fig. 1(e). Figure 1(b)-(d) present the simulated electric field intensity evolution of the MZIs exposed in air based on beam propagation method. These figures show the spatial distribution of light power in the meridian plane as the light propagates through the proposed structure, and the energy flux could be described by the Poynting vector of the light wave. The

simulation results of the MAMZIs with different lateral offsets indicate that light interference occurs between the two branches of light beams respectively propagating though the microfiber and the fiber cavity. Typical parameters of Corning SMF-28e fiber with the relative refractive difference Δn of 0.36% and cladding refractive index of 1.444 at λ=1.55 μm are adopted in our simulation process. Owing to the existence of the large lateral offset, the guided core mode would split into two parts at the first splicing joint with almost half of the input light

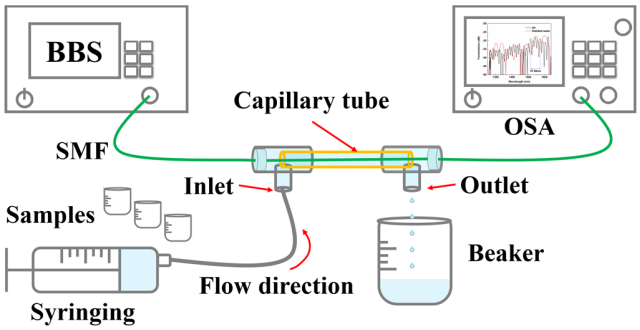

Fig. 3. Schematic diagram of the proposed MAMZI-based microfluidic sensing system.

energy dissipating into the air environment. And eventually, the two branches of light would interfere at the second splicing joint in the presence of the optical path difference between them.

In order to better understand the sensing properties of our proposed MAMZI, the transmission spectral of the three MAMZIs are numerically simulated with ambient environmental RI ranging from 1.33 to 1.3325, as shown in Fig. 2(a)-(c). It could be found that the transmission spectra for the cavities of 351.82 μm and 242.56 μm in length turn out quasi-sinusoidal form compared to their sinusoidal counterparts for the 181.31-μm-long cavity, which means that the transmission spectral intensity of the longer cavity could no longer be analysed with the dual mode interference model due to the presence of high-order modes. From Fig. 2(d), it could be found that the RI sensitivities of the three MAMZIs are 5620 nm/RIU, 9080 nm/RIU and 11680 nm/RIU, respectively. It should be noted that the proposed interferometer with shorter cavity length possesses higher RI sensitivity.

III. Experimental Results and Discussion

Seven series of NaCl solutions of 0 wt% to 3 wt% with a solution interval of 0.5 wt% is prepared at room temperature to serve as the fluid analyst for the experiment. Figure 3 schematically depicts the proposed MAMZI-based microfluidic sensing system for the measurement of fluid sample solution. During the whole experimental process, the environmental temperature is kept at about 24.5 ℃. A broadband source (BBS) is utilized to provide input light with wavelength ranging from 1250 to 1640 nm, and its maximum light intensity is -30 dBm. The transmission spectrum is monitored in real time by using an optical spectrum analyser (OSA: Yokogawa AQ6370C, Japan) whose operation wavelength range and wavelength resolution are 600-1700 nm and 0.1 nm, respectively. We encapsulate the MAMZI structure into a capillary tube with several millimeters in length and employ two plastic T-shaped tubes to respectively work as the inlet and outlet of the microfluidic cell. The inner diameters of capillary and T-shaped tubes are about 300 μm and 500 μm, respectively. In order to prevent possible leakage of liquid sample from the microfluidic cell, the spacing between capillary and T-shaped tubes is sealed with paraffin. The liquid sample is pressurized into the microfluidic cell by utilizing a syringing pump, and a beaker is placed proximity to the outlet to collect the discharge liquid. The consumption of liquid sample is low to microliters according to the size of microfluidic cell mainly constructed by the capillary tube.

The transmission spectral properties of the microfluidic sensing system based on three different MAMZI structures have been experimentally investigated, as shown in Fig 4. We pump NaCl solutions with different concentrations ranging from 0 to 3 wt% into the microfluidic cell in sequence at a constant flowing speed of 5 mL/min. And for the purpose of improving the accuracy of the experimental results as much as possible, we clean the microfluidic channel with distilled water for 2 or 3 times before the next NaCl solution sample is reloaded. Savitzky-Golay filter based on the method of linear least squares [29] is adopted to low down the spectral noises in the experimentally obtained transmission spectra. Fig. 4(a)-(c) give transmission spectra of the three MAMZIs in air and distilled water environments, respectively. Owing to the light scattering

TABLE I
A COMPARISON OF SENSING PROPERTIES FOR TYPICAL WAVELENGTH-INTERROGATED FIBER SALINITY SENSORS WITH OUR PROPOSED MAMZI.

Sensor type	Probe size	Sensitivity	Concentration range	Fiber modification method	References
FBG	1 cm	0.0165 nm/M	0-33.31 wt%	Polymer coating	12
LPG-based MZI	7.38 cm	0.3867 nm/M	0-15 wt%	-	13
TFBG	~ cm	5.6651 nm/M	0-26 wt%	-	14
LPG	5 cm	36 nm/M	0.58-4.68 wt%	polyelectrolyte coating	15
Fiber Sagnac interferometer	~ cm	0.742 nm/M	0-29.2 wt%	Polymer coating	16
Twin-core-fiber-based sensor	5 cm	14.0086nm/M	0-29.2 wt%	-	17
Multimodal fiber sensor	~ cm	1.1308 nm/M	3.86-21.62 wt%	-	18
Microfiber knot resonator		1.2390 nm/M	2-3.7 wt%	-	21
PCF	1.12 cm	88.218 nm/M (15.08 nm/%)	0-2 wt%	-	25
MAMZI	351.82 μm	141.51 nm/M (24.19 nm/%)	0-3 wt%	-	Our work

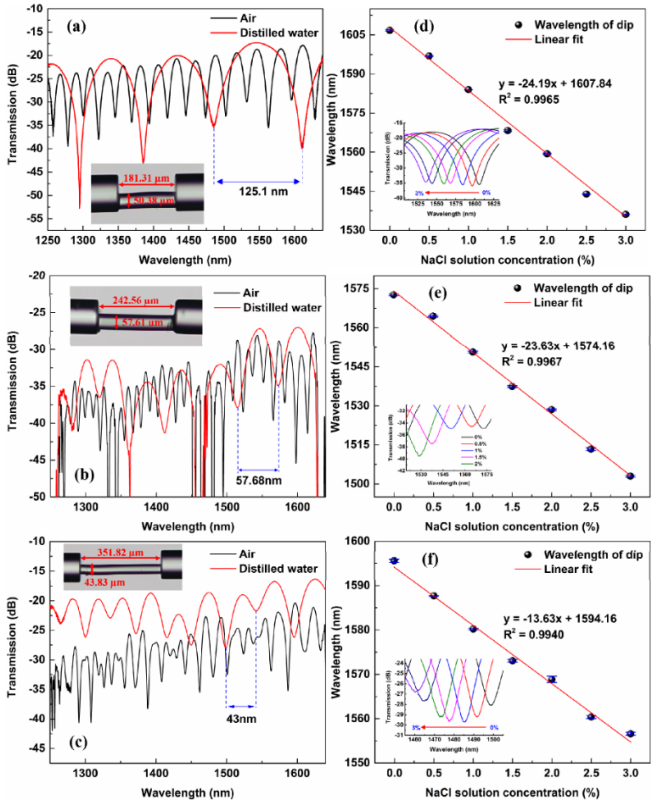

Fig. 4 (a)-(c) Transmission spectra of the fabricated MAMZIs in air and distilled water environment for cavity lengths of 181.31 μm, 242.56 μm and 351.82 μm, respectively; (d)-(f) Transmission dip wavelength as functions of NaCl solution concentration for cavity lengths of 181.31 μm, 242.56 μm and 351.82 μm, respectively.

effect of air, the fiber interferometer with longer cavity length experiences larger transmission loss. When pumping distilled water into the microfluidic channel, it should be noted that the whole transmission loss of all of the three interferometers decreases, which results from better light confinement of the U-shaped micro-cavity immersed into distilled water in comparison with air environment. And compared to the transmission spectrum of the MAMZI of 181.31 μm in length, the MAMZI of 351.82 μm in length exhibits more irregular transmission dips in air environment, which indicates that high-order fiber modes would be involved in light interference due to the increment of interference length. However, the transmission spectra of the three MAMZIs turn out regular transmission dips in distilled water environment, which could be explained by the fact that some higher-order modes would no longer be coupled back at the second splicing due to the increment of micro-cavity RI. According to Eq. (2), the free spectral range (FSR) of the proposed interferometer could be calculated by using $\Delta\lambda = \lambda_1\lambda_2 / \Delta n_{eff} L$ [30]. It should be noted that the FSR is inversely proportional to the interference length and Δn_{eff} . Due to the trivial environmental temperature fluctuation, the thermal-expansion and thermal-optic effects of the silica-based microfiber could be actually neglected according to our previous experimental results reported in Ref. 27. It could be found that the FSRs of the three MAMZIs with

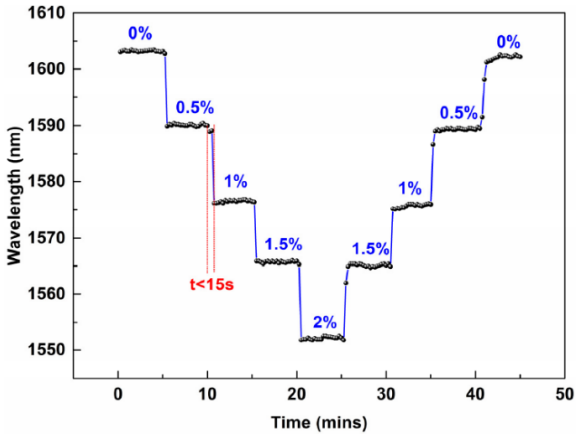

Fig. 5. Real-time response of transmission dip wavelength with respect to the variation in NaCl solution concentration.

different cavities lengths of 181.31 μm, 242.56 μm and 351.82 μm are 125.1 nm, 57.68 nm and 43 nm, respectively, which agrees well with our theoretical analysis. Fig. 4(d)-(f) show wavelength shift of selected transmission dips as functions of NaCl solution concentration for different MAMZI structures. All of the transmission spectra are recorded for five times to evaluate the wavelength fluctuations induced by random experimental error. The error bars in Figure 4 indicates that the wavelength fluctuations are located within acceptable range. The inset graphs show the transmission spectral evolution of the MAMZIs with cavity lengths of 351.82 μm, 242.56 μm and 181.31 μm for different NaCl solution concentrations. It could be found that all of the three MAMZIs show wavelength shift toward shorter wavelength region as the concentration of NaCl solution gradually increases from 0 to 3 wt%. And the wavelength sensitivities of the three MAMZs reach -24.19 nm/ (1 wt%), -23.63 nm/ (1 wt%) and -13.63 nm/ (1 wt%), respectively. The above experimental measurement results come to the conclusion that the proposed MAMZI with shorter cavity length possesses higher RI sensitivity, which is in good consistency with the previous simulated results in this article. On account of the optical spectrum analyzer (OSA) with the wavelength resolution of 0.1 nm utilized in the experiment, the minimum concentration detection limit of NaCl solution is as low as 4×10^{-3} wt%. At given temperature and atmospheric pressure, the refractive index of NaCl solution is a single-valued function of the solution concentration. The RI variation of NaCl solution is about 1.5×10^{-3} for a concentration change of 1 wt% [25]. Consequently, the RI sensitivity of our proposed interferometer is up to 10^4 nm/RIU. It should be noted that the temperature dependences of the proposed MAMZI in air and distilled water environments are respectively about 0.04619 nm/°C and 1.4633 nm/°C according to our previous work [27]. Considering the wavelength shift sensitivity of tens of nanometers per 1 wt% and the low temperature fluctuation during the whole experimental process, the temperature effect could be actually neglected.

A comparison of sensing properties for the typical wavelength-interrogated fiber salinity sensors reported in

previous studies and the one proposed in our study is listed in Table 1. It is obvious that the proposed MAMZI has salinity sensitivities significantly higher than its counterparts based on optical fiber gratings or interferometric fiber sensors, and its salinity sensitivities are comparable to those of the PCF-based schemes. Moreover, the proposed sensing probe does not require complex polymer coating procedure for fiber surface modification and it has a compact structure of a few hundred micrometers in length, which makes it well compatible with highly integrated measurement systems for trace analysis of microfluidic samples.

To evaluate the time response feature of our proposed microfluidic sensing system, transmission spectra are recorded every 15 seconds during a 45-minute time span in which NaCl solutions with different concentrations ranging from 0 to 2 wt% with an constant interval of 0.5 wt% are circularly pumped into the microfluidic cell. Fig. 5 shows the central wavelength of a selected transmission dip in real-time response to the change of NaCl solution concentration. It could be found that the response time is less than 15 s for one single solution test.

IV. Conclusions

In summary, a MAMZI-based microfluidic sensing system for real-time salinity measurement of aqueous solution samples. The proposed fiber interferometer is fabricated by splicing a microfiber of several hundred micrometers in length with two standard SMFs with pre-designed lateral offset have been proposed and experimentally demonstrated. Three MAMZIs of 351.82 μm, 242.56 μm and 181.31 μm in cavity lengths have been fabricated and their transmission properties have been theoretically as well as experimentally investigated. Experimental results show that the wavelength sensitivities of the three MAMZs are -13.63 nm/ (1 wt%), -23.63 nm/ (1 wt%), and -24.19 nm/ (1 wt%), respectively. Considering its outstanding advantages such as utra-high RI sensitivity up to 105 nm/RIU, ultra-short cavity length of several hundred micrometers and fast response time of less than 15 s, our proposed fiber interferometer is anticipated to find practical uses in related label-free chemical and biological detection applications.

References

[1] D. Psaltis, S. R. Quake, and C. Yang, "Developing optofluidic technology through the fusion of microfluidics and optics," *Nature,* vol. 442, no. 7101, pp. 381-386, 2006.

[2] C. Monat, P. Domachuk, and B. J. Eggleton, "Integrated optofluidics: A new river of light," *Nature Photonics,* vol. 1, no. 2, pp. 106-114, 2007.

[3] X. Fan and I. M. White, "Optofluidic Microsystems for Chemical and Biological Analysis," *Nature Photonics,* vol. 5, no. 10, pp. 591-597, 2011.

[4] L. Pang, H. M. Chen, L. M. Freeman, and Y. Fainman, "Optofluidic devices and applications in photonics, sensing and imaging," *Lab on A Chip,* vol. 12, no. 19, pp. 3543-3551, 2012.

[5] A. Ymeti *et al.*, "Integration of microfluidics with a four-channel integrated optical Young interferometer immunosensor," *Biosensors & Bioelectronics,* vol. 20, no. 7, pp. 1417-1421, 2005.

[6] A. Crespi *et al.*, "Three-dimensional Mach-Zehnder interferometer in a microfluidic chip for spatially-resolved label-free detection," *Lab on A Chip,* vol. 10, no. 9, pp. 1167-1173, 2010.

[7] M. I. Lapsley, I. K. Chiang, Y. B. Zheng, X. Ding, X. Mao, and T. J. Huang, "A single-layer, planar, optofluidic Mach–Zehnder interferometer for label-free detection," *Lab on A Chip,* vol. 11, no. 10, pp. 1795-1800, 2011.

[8] Y. Guo, M. K. K. Oo, K. Reddy, and X. Fan, "Ultrasensitive Optofluidic Surface-Enhanced Raman Scattering Detection with Flow-through Multihole Capillaries," *Acs Nano,* vol. 6, no. 1, pp. 381, 2012.

[9] Y. Zhao, X. Zhang, T. Zhao, B. Yuan, and S. Zhang, "Optical Salinity Sensor System Based on Fiber-Optic Array," *IEEE Sensors Journal,* vol. 9, no. 9, pp. 1148-1153, 2009.

[10] H. Z. Yang, X. G. Qiao, K. S. Lim, and S. W. Harun, "Optical Fiber Sensing of Salinity and Liquid Level," *IEEE Photonics Technology Letters,* vol. 26, no. 17, pp. 1742-1745, 2014.

[11] H. A. Rahman, S. W. Harun, M. Yasin, and H. Ahmad, "Fiber optic salinity sensor using beam-through technique," *Optik - International Journal for Light and Electron Optics,* vol. 124, no. 8, pp. 679-681, 2013.

[12] L. Men, P. Lu, and Q. Chen, "A multiplexed fiber Bragg grating sensor for simultaneous salinity and temperature measurement," *Journal of Applied Physics,* vol. 103, no. 5, pp. 5267, 2008.

[13] G. R. C. Possetti, R. C. Kamikawachi, C. L. Prevedello, M. Muller, and J. L. Fabris, "Salinity measurement in water environment with a long period grating based interferometer," *Measurement Science & Technology,* vol. 20, no. 3, pp. 034003, 2009.

[14] W. Zhou, D. J. Mandia, S. T. Barry, and J. Albert, "Absolute near-infrared refractometry with a calibrated tilted fiber Bragg grating," *Optics Letters,* vol. 40, no. 8, pp. 1713, 2015.

[15] F. Yang, S. Sukhishvili, H. Du, and F. Tian, "Marine Salinity Sensing Using Long-period Fiber Gratings Enabled by Stimuli-responsive Polyelectrolyte Multilayers," *Sensors & Actuators B Chemical,* vol. 253, pp. 745-751, 2017.

[16] C. Wu, B. O. Guan, C. Lu, and H. Y. Tam, "Salinity sensor based on polyimide-coated photonic crystal fiber," *Optics Express,* vol. 19, no. 21, pp. 20003-20008, 2011.

[17] J. R. Guzman-Sepulveda, V. I. Ruiz-Perez, M. Torres-Cisneros, J. J. Sanchez-Mondragon, and D. A. May-Arrioja, "Fiber Optic Sensor for High-Sensitivity Salinity Measurement," *IEEE Photonics Technology Letters,* vol. 25, no. 23, pp. 2323-2326, 2013.

[18] Q. Meng, X. Dong, K. Ni, and Y. Li, "Optical Fiber Laser Salinity Sensor Based on Multimode Interference Effect," *IEEE Sensors Journal,* vol. 14, no. 6, pp. 1813-1816, 2014.

[19] M. F. Jaddoa, A. A. Jasim, M. Z. A. Razak, S. W. Harun, and H. Ahmad, "Highly responsive NaCl detector based on inline microfiber Mach–Zehnder interferometer," *Sensors & Actuators A Physical,* vol. 237, pp. 56-61, 2016.

[20] H. A. Rahman *et al.*, "Tapered plastic multimode fiber sensor for salinity detection," *Sensors & Actuators A Physical,* vol. 171, no. 2, pp. 219-222, 2011.

[21] Y. Liao, J. Wang, H. Yang, X. Wang, and S. Wang, "Salinity sensing based on microfiber knot resonator," *Sensors & Actuators A Physical,* vol. 233, pp. 22-25, 2015.

[22] D. J. Gentleman and K. S. Booksh, "Determining salinity using a multimode fiber optic surface plasmon resonance dip-probe," *Talanta,* vol. 68, no. 3, pp. 504-515, 2006.

[23] N. Díazherrera, O. Esteban, M. C. Navarrete, M. Lehaitre, and A. Gonzálezcano, "In situ salinity measurements in seawater with a fibre-optic probe," vol. 17, no. 8, pp. 2227-2232(6), 2006.

[24] Z. He, Y. Zhu, and H. Du, "Long-period gratings inscribed in air- and water-filled photonic crystal fiber for refractometric sensing of aqueous solution," *Applied Physics Letters,* vol. 92, no. 4, pp. 1193, 2008.

[25] C. Wu *et al.*, "In-line microfluidic integration of photonic crystal fibres as a highly sensitive refractometer," *Analyst,* vol. 139, no. 21, pp. 5422-5429, 2014.

[26] S. Gao, W. Zhang, H. Zhang, and C. Zhang, "Reconfigurable and ultra-sensitive in-line Mach-Zehnder interferometer based on the fusion of microfiber and microfluid," *Applied Physics Letters,* vol. 106, no. 8, pp. 289, 2015.

[27] N. Xie, H. Zhang, B. Liu, J. Wu, B. Song, and T. Han, "Highly sensitive in-line microfluidic sensor based on microfiber-assisted Mach-Zehnder interferometer for glucose sensing," *Journal of Optics,* vol. 19, no. 11, pp. 115803, 2017.

[28] N. Xie, H. Zhang, B. Liu, B. Song, and J. Wu, "Characterization of temperature-dependent refractive indices for nematic liquid crystal

employing microfiber-assisted Mach-Zehnder interferometer," Journal of Lightwave Technology, vol. 35, no. 14, pp. 2966-2972, 2017.
[29] A. Savitzky and M. J. E. Golay, "Smoothing and Differentiation of Data by Simplified Least Squares Procedures," *Analytical Chemistry,* vol. 36, no. 8, pp. 1627-1639, 1964.
[30] C. H. Chen, W. T. Wu, and J. N. Wang, "All-fiber microfluidic multimode Mach–Zehnder interferometers as high sensitivity refractive index sensors," *Microsystem Technologies,* vol. 23, no. 2, pp. 1-12, 2017.

Nanjie Xie received the Bachelor's degree in applied physics in 2015 from Central South University of Forestry and Technology, China. He is currently a Master degree candidate in optical engineering at Institute of Modern Optics, Nankai University. His research interests are mainly focused on novel fiber sensors based on micro/nano fiber structures and functional fiber-optic components.

Hao Zhang received the Ph.D. degree in optics from Nankai University, China, in 2005. He is currently a professor at Institute of Modern Optics, Nankai University. His research interests include micro/nanostructured fiber devices, novel fiber sensors, and fiber lasers.

Bo Liu received the Ph.D. degree in optics from Nankai University, China, in 2004. He is currently a professor at Institute of Modern Optics, Nankai University. His research interests include fiber sensors, fiber-grating-based photonic devices, and interrogation systems.

Haifeng Liu received the Ph.D. degree in Optics from Nankai University, China, in 2016. He is currently an engineer at Institute of Modern Optics, Nankai University. His research interests include novel fiber-optic devices based on functional materials and their applications.

Ting Liu received the Bachelor's degree in optoelectric information science and engineering in 2017 from Wuhan Institute of Technology, China. She is currently a Master degree candidate in optical engineering at Institute of Modern Optics, Nankai University. Her research interests include fiber-optic sensing technology.

Chao Wang received the Ph. D. degree in Electrical and Computer Engineering from University of Ottawa, Canada, in 2011. He is currently a Senior Lecturer in the School of Engineering and Digital Arts, University of Kent, UK. His research interests lie in inter-disciplinary areas that study the interaction between Photonics and other traditional or state-of-the-art technologies in different fields, such as microwave photonics, optical communications, and biophotonics for widespread industrial, communications, biomedical and defense applications.